IV International Conference on Particle-based Methods – Fundamentals and Applications
PARTICLES 2015
E. Oñate, M. Bischoff, D.R.J. Owen, P. Wriggers & T. Zohdi (Eds)

REGULAR OR RANDOM: A DISCUSSION ON SPH INITIAL PARTICLE DISTRIBUTION

J. YOUNG, I. ALCÂNTARA, F. TEIXEIRA-DIAS, J. OOI AND F. MILL

School of Engineering
The University of Edinburgh
The King's Buildings, Edinburgh EH9 3JL, UK
E-mail: james.young@ed.ac.uk (corresponding author), URL: http://www.eng.ed.ac.uk/

Key words: Smooth particle hydrodynamics, Initial particle distribution, Random particle distribution, Lid driven cavity, Flow

Abstract. Smoothed Particle Hydrodynamics (SPH) has been used to model a variety of objects and for a number of applications in engineering and science. These have ranged from astrophysics to fluid and solid mechanics problems. Much research has been dedicated to forming a better understanding of the SPH method. As a consequence, new numerical techniques have been developed in order to overcome some of its difficulties and limitations. Nonetheless, there is still a gap in information concerning the impact of the initial particle distribution on the effectiveness of the SPH method. With this in mind, a review of existing recommendations for SPH initial configurations has been conducted in this paper. In addition to this, a numerical example is presented which is based on the classical 2-D lid driven cavity problem, wherein the upper boundary exerts a horizontal shear force on the fluid inside the cavity. The velocity of the lid is $v = 10^{-3}$ m/s and the cavity is square with length $l = 1x10^{-3}$ m. The fluid was modelled with a density $\rho = 1000$ kg/m^3, a viscosity $\mu = 10^{-3}$ kg/ms) (Re = 1). These parameters were held constant for all consequent comparisons. The number of particles is varied from (20 $\times$ 20) to (80 $\times$ 80). The initial distribution is modelled in three different ways: (i) regular, (ii) pseudo-random (with a 30% random deviation from the regular grid) and (iii) fully random. The effectiveness of each initial particle distribution is assessed according to the field velocities and horizontal and vertical centreline velocity profiles. The impact of the initial particle distribution is highlighted and compared against a reference CFD result, and recommendations and conclusions are drawn for the SPH method.

1 INTRODUCTION

In recent years, new numerical techniques have been developed in order to overcome some of the difficulties and limitations inherent to the SPH method. Despite this progression, there is still a gap in information concerning the impact of initial particle distribution. A literature review highlighted that most SPH simulations implement a completely regular initial particle distribution. With this in mind, a review of existing methods in SPH initial configurations has been conducted.

Idelshon et al. [1] discussed various essential issues concerning meshless methods and, in particular, what is meaningful when opting for a non-mesh-based method over a mesh-based one. However, the authors don't focus specifically on the impact of initial particle distribution in meshless methods.

Diehl et. al. [2] present a novel, and perhaps the most comprehensive, study on the effect of initial particle spacing on SPH. In comparing initial particle distributions the authors highlight that a cubic lattice arrangement is prone to artefacts due to the alignment of particles along grid axes although it does display very little noise and is simple to implement. They do not recommend this method. Similarly, random initial configurations are not recommended as the lattice effects are not fully understood and the configuration results in high levels of noise. The authors propose an initial configuration based on Weighted Voronoi Tessellations (WVTs), which has been implemented in a variety of astrophysics problems. They further present a new method for setting up SPH simulations with arbitrary, spatially varying resolution requirements in 2, 3 or N dimensions. While discussing the difficulties in estimating the errors in the SPH equations from first principles, Monaghan [3] states that these errors depend on the dynamics of the simulation. He further states that one approach to estimate these errors involving initially distributing the particles on a regular grid and then shifting them randomly by some distance, as investigated by Colagrossi [4]. Monaghan goes on to state that if the particle spacing is small relative to the dominant length scales, then the disorder resulting from the initial shifting of particles is not relevant.

Monaghan [5] later wrote a paper addressing the claims by Imaeda et al. [6] that the SPH method contains a fundamental flaw which is highlighted by shear flow simulations. Monaghan's paper stated that, provided that the initial particles configuration was in an equilibrium state, the results obtained were independent of initial distribution. Monaghan also highlights how, for for simulations with a low Mach number and stiff equations of state, the initial particle distribution equilibrium condition is of paramount importance. If this condition is not respected and particles are placed at random, Monaghan states that "violent fluctuations in the pressure will drive the fluid out of the region of interest".

While discussing the importance of local conservation, Price [7] states how a random initial distribution will result in errors which are proportional to $1/\sqrt{N}$, where N is the number of particles in the simulation. Price continues to demonstrate that, in a Hamiltonian system, the particles will rearrange until a minimum energy state is achieved, thus leading to an inherent re-meshing of particles. Cartwright et al. [8] investigated the effect of Poisson noise on simulations involving rings of particles in Keplerian rotation. This Poisson noise was a product of using a random number algorithm in the initial placement of particles, which is commonly found in simulations involving spiral galaxies. This investigation highlighted that gravity calculations are not affected by Poission noise. Density was found to be much more susceptible and the effect increased with the total number of particles. The pressure calculations were found to be the most influenced by noise where the effect was found to scale with $\sqrt{N}$. Hubber et al [9] confirm the Poissonian errors given by both Price and Cartwright. They further state that as the minimum energy state, as discussed previously, is formed, the errors in the corresponding lattice distribution scales with $1/(N \log N)$.

Controlling the initial particle distribution appears to fundamentally conflict with the philosophy of the SPH method. A large number of authors agree that best results are achieved when avoiding a fully random initial particle distribution, provided they are not relaxed prior to running the simulation.

A numerical example based on a 2D shear driven cavity problem is examined in the present paper in order to highlight the effect of initial particle distribution. The numerical example uses a variety of initial particle distributions including; completely random, pseudo-random and regular distributions. The aim of the numerical example is to aid in determining some generic conclusions about the influence of initial particle distribution on the SPH method.

2 SMOOTHED PARTICLE HYDRODYNAMICS

Initially devised to solve astrophysical problems in three-dimensional open space [10, 11], smoothed particle hydrodynamics is considered to be a truly meshfree particle method and one of the oldest of its kind. Since its initial formulation, SPH has been extended to a range of physical problems including fluid and solid mechanics. The collective movement of the particles resembles the movement of a liquid or a gas flow and it can be modelled using equations from classical Newtonian hydrodynamics. A basic SPH formulation is presented below. A more detailed formulation can be found in [12, 13, 14].

2.1 General SPH formulation

In SPH, a system is represented by a set of particles which are distributed throughout the continuum. These particles posses material properties and interact with each other depending on their range of influence which is controlled by a weighting or smoothing function. The particles require no connectivity. Field functions are first converted into their integral representation. This also known as the kernel approximation. The kernel approximation of a function $f(x)$ is represented by the integration of the multiplication of that function by the smoothing kernel function.

$$\langle f(x)\rangle = \int_{\Omega} f\left(x'\right)\nabla W\left(x - x', h\right) \mathrm{d}x' \tag{1}$$

Within the smoothing kernel function, or smoothing function, h is the smoothing length which is used to define the area of influence of the smoothing function W. This smoothing function should fulfil some basic requirements [15, 16]. The approximation for the spatial derivative $\langle\nabla \cdot f(x)\rangle$ is obtained by substituting $f(x)$ with $\langle\nabla \cdot f(x)\rangle$ in equation 1 and applying the divergence theorem along with the knowledge that the surface integration can be neglected inside the problem domain, which gives

$$\langle\nabla \cdot f(x)\rangle = -\int_{\Omega} f(x') \cdot \nabla W(x - x', h)\mathrm{d}x' \tag{2}$$

The kernel approximation is then further estimated through particles, which is known as the particle approximation. This is achieved by replacing the integration in the representation of the field function and its derivatives with summations over all the correlating values at the neighbouring particles in a local domain called the support domain. The particle approximation of a field function is given as

$$\langle f(x)\rangle = \sum_{j=1}^{N} \frac{m_j}{\rho_j} f\left(x_j\right) \cdot \nabla W_{ij} \qquad \text{where} \qquad \nabla W_{ij} = \frac{x - x'_j}{r_{ij}} \frac{\delta W_{ij}}{\delta r_{ij}} = \frac{x_{ij}}{r_{ij}} \frac{\delta W_{ij}}{\delta r_{ij}} \tag{3}$$

N is the total number of particles within the influence area of the particle i. Similarly, the particle approximation of the derivative of a field function is given by

$$\langle \nabla \cdot f(x)\rangle = -\sum_{j=1}^{N} \frac{m_j}{\rho_j} f\left(x_j\right) \cdot \nabla W_{ij} \tag{4}$$

The values of the particle approximations are calculated at every time step. Therefore, the distribution of particles may initially influence the results. The formulation described is applied to field functions in the form of partial differential equations (PDEs) and results in ordinary differential equations (ODEs) in a discretized form which is dependent on time. The ODEs are solved through an explicit integration algorithm in order to achieve fast time stepping.

2.2 SPH formulation of the Navier-Stokes equations

The SPH formulation of the Navier-Stokers equations is derived by firstly discretising the equations. This leads to a set of ODEs which evolve with time. This set of ODEs can then be solved through time integration and are based on three fundamental physical laws of conservation: conservation of mass, conservation of momentum and conservation of energy. By implementing the general formulation given above, the Navier-Stokes equations can be written as [12, 14]

$$\begin{cases} \dfrac{D\rho_i}{Dt} = \displaystyle\sum_{j=1}^{N} m_j {v^{\beta}}_{ij} \cdot \frac{\partial W_{ij}}{\partial {x^{\beta}}_i} \\ \dfrac{D{v_i}^{\alpha}}{Dt} = -\displaystyle\sum_{j=1}^{N} m_j \left(\frac{{\sigma^{\alpha\beta}}_i}{\rho_i^2} + \frac{{\sigma^{\alpha\beta}}_j}{\rho_j^2} \right) \frac{\partial W_{ij}}{\partial {x^{\beta}}_i} \\ \dfrac{De_i}{Dt} = \dfrac{1}{2} \displaystyle\sum_{j=1}^{N} m_j \left(\frac{p_i}{\rho_i^2} + \frac{p_j}{\rho_j^2} \right) {v^{\beta}}_{ij} \frac{\partial W_{ij}}{\partial {x^{\beta}}_i} + \frac{\mu_i}{2\rho_i} \varepsilon_i^{\alpha\beta} \varepsilon_i^{\alpha\beta} \\ \dfrac{D{x_i}^{\alpha}}{Dt} = v_i^{\alpha} \end{cases} \tag{5}$$

where σ is the total stress tensor made up of isotropic pressure and viscous stress such that $\sigma^{\alpha\beta} = -p\delta^{\alpha\beta} + \tau^{\alpha\beta}$ and $\tau^{\alpha\beta} = \mu\varepsilon^{\alpha\beta}$, where μ is the dynamic viscosity and ε is the shear strain rate. The relative velocity between particles, $v_{ij} = v_i - v_j$. The Greek subscripts α and β denote coordinate directions and summations in the discretised equations are taken over repeated indices.

3 NUMERICAL MODEL

The numerical example presented is based on a 2D lid driven cavity problem, where the upper boundary exerts a horizontal shear force on the fluid in the cavity. The purpose of this example was to highlight and compare the impact of initial particle distributions. The example is a derivation of that which is presented by Liu [14].

A square ($l = 1 \times 10^{-3}$ m) cavity is filled with water. The bottom and side walls of the cavity are rigid. The top wall, or lid, slides in its plane from left to right at a velocity of 1×10^{-3} m/s exerting a shear force on the fluid within the cavity. The fluid was modelled with a density $\rho = 1000$ kg/m^3 and a viscosity $\mu = 10^{-3}$ kg/ms yielding Re = 1. In addition to these properties, the particles which simulated the fluid were also initialised with zero velocity and pressure. Gravity was neglected.

Three different particle distributions were investigated. These included a completely random distribution, a pseudo-random distribution and a completely regular distribution. Through varying the number of particles in the domain of each test, the sensitivity of the simulation to the number of particles was explored in addition to the impact of initial particle distribution. With this in mind, a total of four different domain particle densities was implemented. The following 12 tests were carried out: three different initial particle distributions, each with four different number of particles. Particle distributions varied from completely random to pseudo-random to regular. The number of particles varied from 400 (20×20) to 1600 (40×40), 3600 (60×60) and 6400 (80×80), excluding virtual or boundary particles. The same number of particles was used for the random and partly random configurations to model the fluid.

The pseudo-random configuration was created by shifting each particle in the regular grids randomly by up to 30% of the spacing between particles. This ensured that an element of disorder was incorporated into the initial distribution whilst preventing the particles from clumping together.

The cavity walls and lid were modelled using virtual particles that exert a repulsive boundary force on the inner particles to prevent them from escaping the domain, also known as type 1 particles. The repulsive force was scaled with the particle spacing [14]. For each type of distribution and number of particles, the particles used to model the fluid were offset from the boundary by half the spacing between particles used the in the corresponding regular grid. This was done to prevent the simulation exploding due to the repulsive fore exerted from the boundary. The boundary particles themselves were separated by half the spacing used for the particles modelling the fluid in the regular grids. The same configuration of boundary particles was used for each type of distribution and scaled accordingly with the total number of particles used to model the fluid. The boundary particles modelling the lid were initialised with a velocity of 1×10^{-3} m/s. The properties and position of the boundary particles did not evolve with time but are used in the approximations carried out at the internal particles. Further exterior boundary particles which can be used to ensure that particle deficiency does not occur near the boundary were not used in these simulations, which may have resulted in some inaccuracy. Figure 1 shows the 12 different initial configurations and highlights the boundary and internal particle configurations discussed. The smoothing length of each particle was set as the initial distance between particles in the regular grid in the horizontal direction, which equals the distance in the vertical direction. The mass of each particle was set to the density times the particle spacing in the horizontal and vertical direction in the regular grid. These smoothing lengths and masses were used for the corresponding pseudo-random and random simulations. Although it was appropriate to assume that the mass of the particles in the regular grid was the density of the particle times the discretized volume of space it influences, applying this mass directly to the pseudo-random and random simulation will have resulted in some non-physical initial density distributions. A constant time step of 2.0×10^{-5} was used. All twelve simulations were ran for 7500 time steps, as this was when the most volatile of them was deemed to have reached a steady state solution.

4 RESULTS AND DISCUSSION

A benchmark was required in order to validate the results obtained using the SPH method. With this in mind, a simulation was run on the Computational Fluid Dynamics (CFD) package STAR-CCM+. This simulation was chosen for comparative purposes as the velocity vectors, vorticity contours and locations of primary vortex it produced were in good agreement with those from previous studies [17, 18]. Figure 2 displays the absolute velocity magnitude difference between the SPH simulations and the the STAR-CCM+ reference case while Figure 3 displays the relative difference. These figures are displayed in increasing number of particles (top to bottom) and increasing the element of randomness (left to right). The first column shows the simulation results for the initially regular distribution, the second for the pseudo-random distirbution and the last for the completely random distribution. Figures 4 and 5 show the non-dimensional vertical velocity profile along the horizontal centreline and the non-dimensional horizontal velocity profile along the vertical centreline, respectively.

Figures 4 and 5 highlight that the results produced from the SPH and CFD methods generally agree. It is clear that for the lower particle distributions, the SPH results deviate as compared to the reference solution. Additionally, these figure show how the initially random and pseudo-random distributions produced noisy curves with large fluctuations. These plots appear to indicate that the high density and structured distribution produces the overall best results

Due to the adaptive nature of the SPH method it should not, supposedly, be affected by the arbitrary distribution of particles. Therefore it was expected that the results may have favoured a specific number of initial particles but would not have been heavily influenced by the type of distribution. However, this was clearly not the case as the results showed that a regular distribution produced the most favourable results for the parameters measured. Due to the repulsive force between particles, random distributions were expected to quickly move to their minimum energy state. Although this repositioning of particles inevitably causes some spurious velocities, it was expected that these would quickly dampen out and not impact the overall

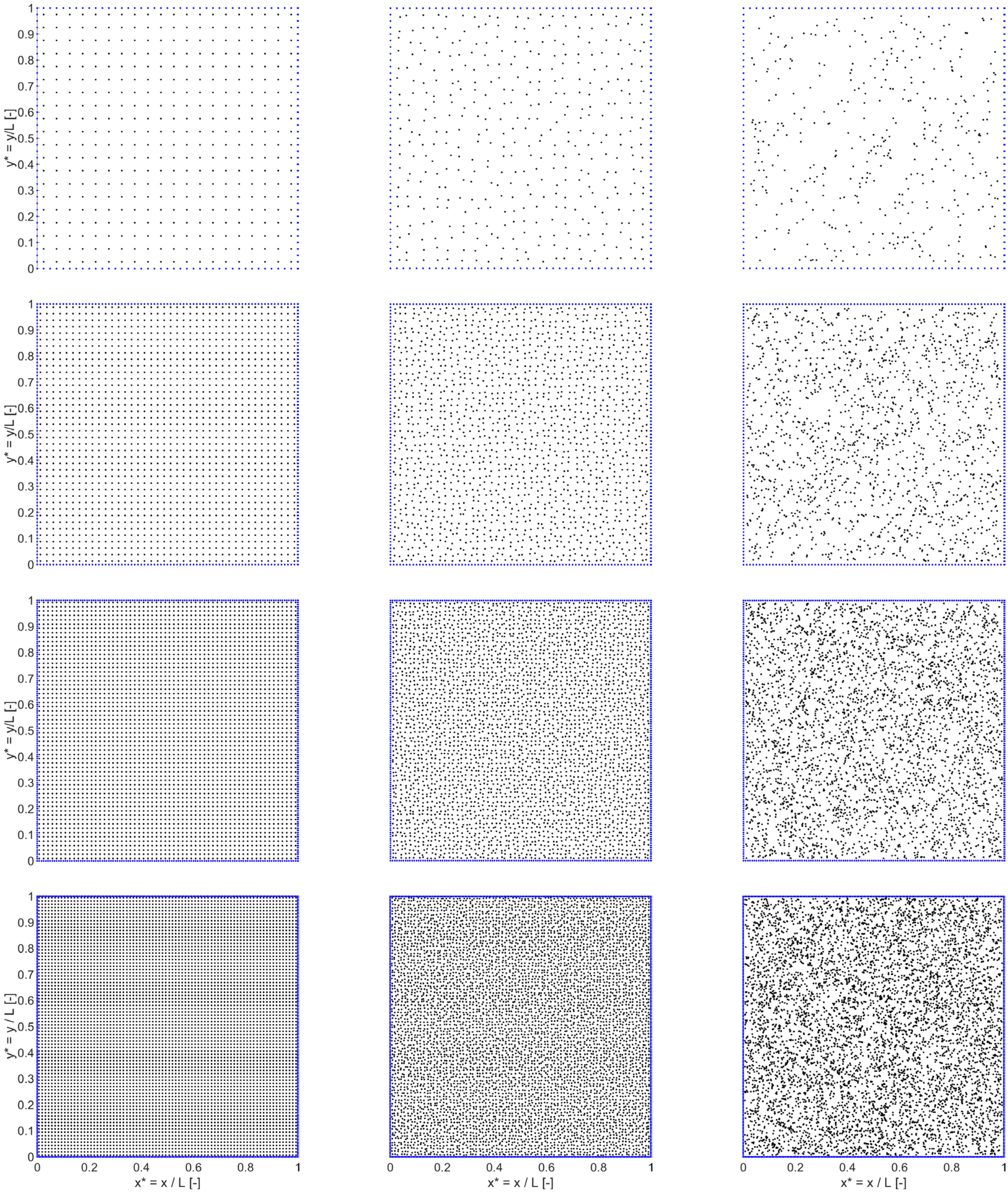

Figure 1: Different particle density for each initial particle distribution: Top to bottom: 20×20, 40×40, 60×60 and 80×80; left to right: regular distribution, pseudo-random distribution and random distribution. Figures 2 and 3 follow this arrangement.

quality of the results.

Figures 2 to 5 clearly highlight that the 20×20 particle distributions simply do not contain a sufficient quantity of particles to accurately capture the physics of the shear cavity. Therefore, when attempting to draw conclusions from the simulation results, these distributions were discarded. The literature review highlighted that a random configuration should not be used unless the distribution is allowed to reach equilibrium prior to imposing external forces. It was predicted that the effects caused by the initially random configuration would be dampened out in the early stages of the simulations. This was checked for the 60×60 random initial configuration which was allowed to reach equilibrium prior to being exposed to the shear force. The results of this simulation did not highlight an improvement over the corresponding simulation which was not allowed to reach equilibrium prior to imposing the shear force.

5 CONCLUDING REMARKS

From the results obtained some general remarks can be made about the influence of the initial particle distribution. The regular distribution produced the least noisy results which were the most easily interpreted. The random distributions were the noisiest of the three which is clearly highlighted by the vertical and horizontal velocity curves around the corresponding centrelines. Although the choice of particle distribution is situational, a regular distribution is recommended. When investigating the number of particles to be used, there is clearly a minimum below which the method cannot capture the physics of the simulation. In the case of this lid-driven shear cavity, that amount was between 400 (20×20) and 1600 (40×40) particles. The results also highlighted that there may also be a recommended maximum number of particles as the transition from 3600 (60×60) to 6400 (80×80) particles resulted in a decrease in the quality of the results obtained, especially for the random configuration. One should also bear in mind the computational costs involved in the simulations. Simulations involving higher number of particles would require more CPU time, while simulations involving lower number of particles would require less CPU time. Additionally, the time used to generate the initial particle configuration should also be accounted for. All the additional factors ought also to be considered when trying to extrapolate conclusions about either to opt for a regular or random distribution, with more or less particle density.

REFERENCES

[1] Idelsohn, S. R. and Oñate, E. To mesh or not to mesh. That is the question... *Comput. Methods in Appl. Mech. Eng.* (2006) **195**(37-40):4681–4696.

[2] Diehl, S. et al. Generating Optimal Initial Conditions for Smooth Particle Hydrodynamics Simulations. *Mon. Not. R. Astron. Soc.* (2012)

[3] Monaghan, J. J. Smoothed particle hydrodynamics. *Rep. Prog. Phys.* (2005) **68**(8):1703–1759.

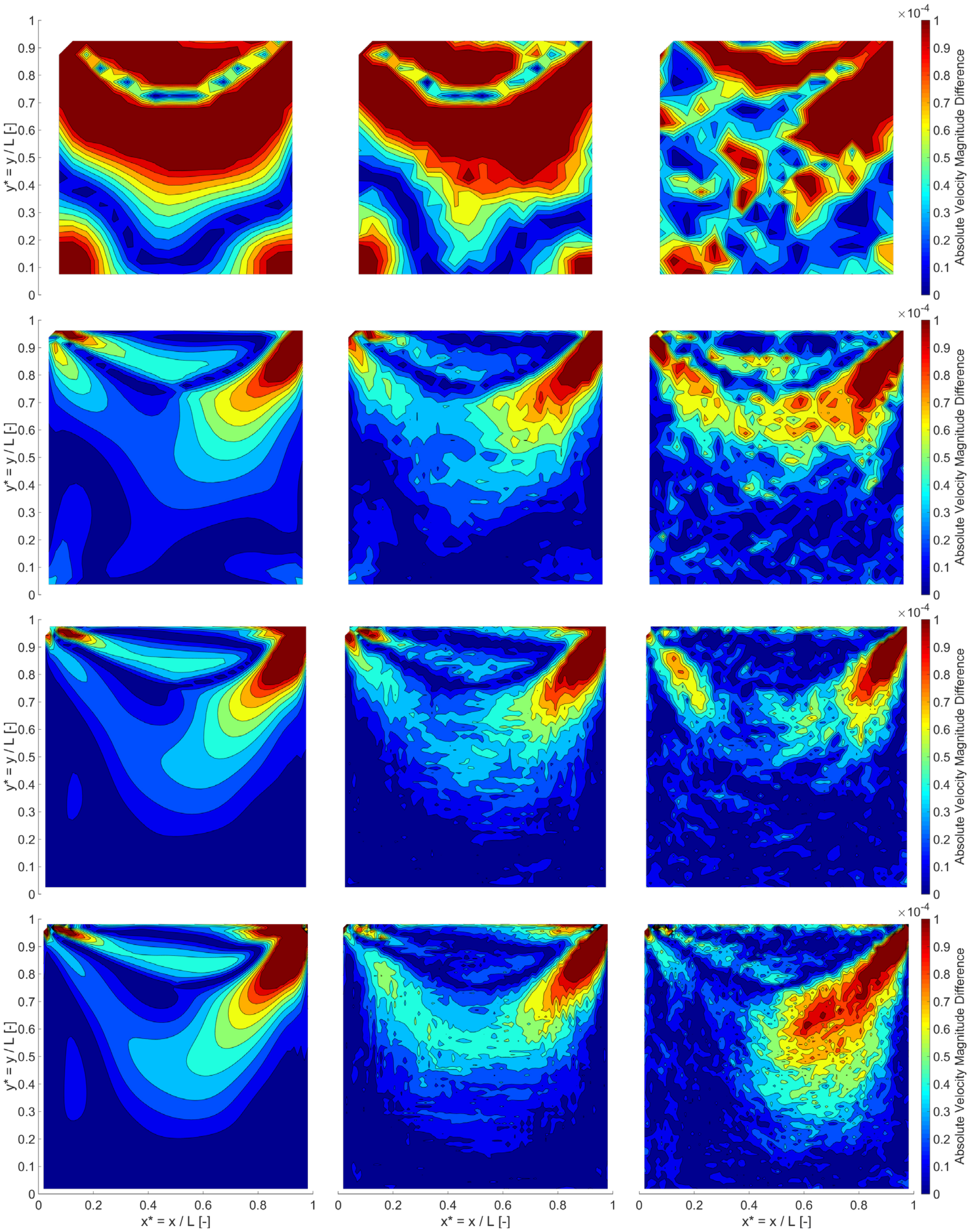

Figure 2: Absolute velocity magnitude difference between SPH results and Star-CM++.

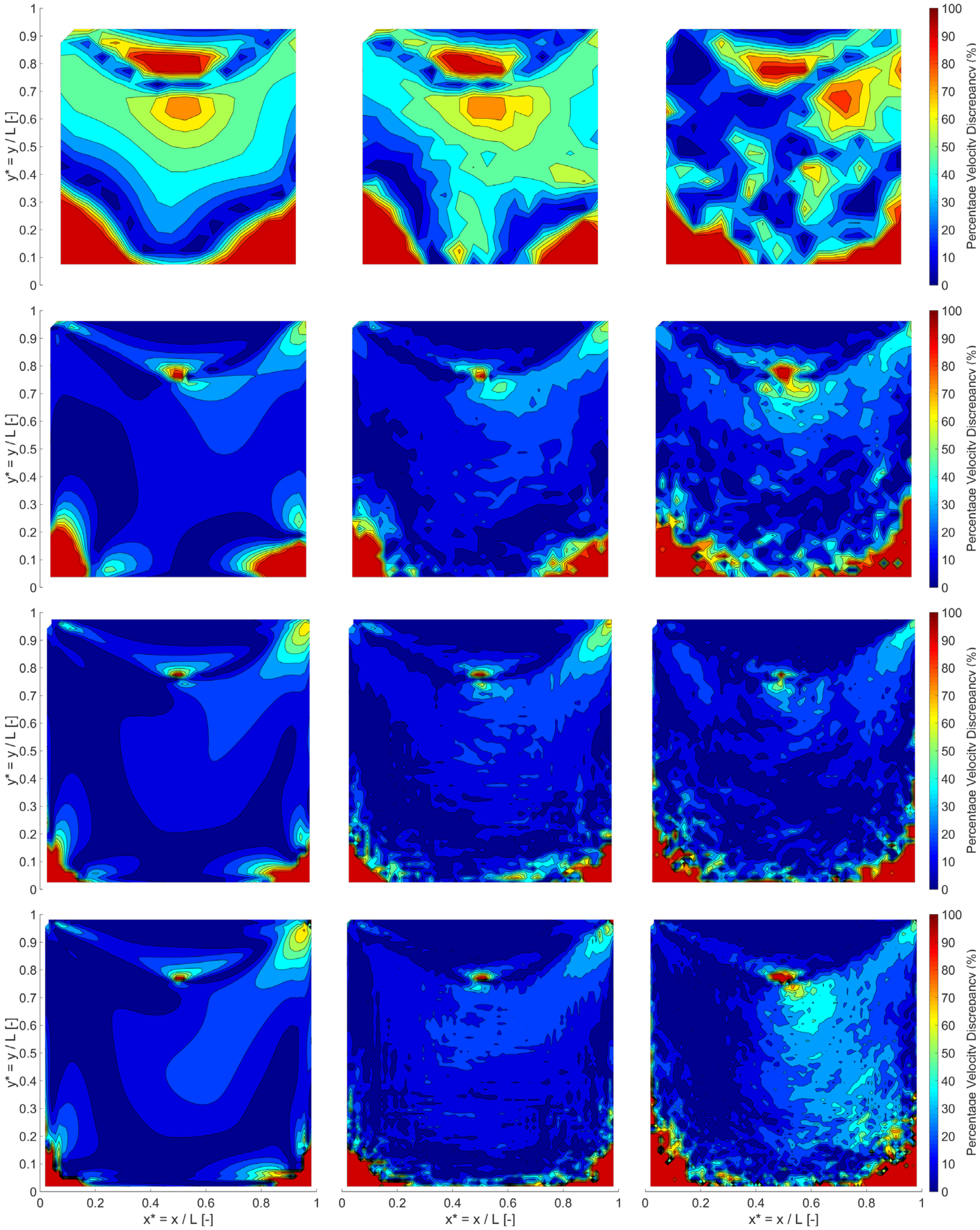

Figure 3: Relative velocity magnitude difference between SPH results and Star-CM++.

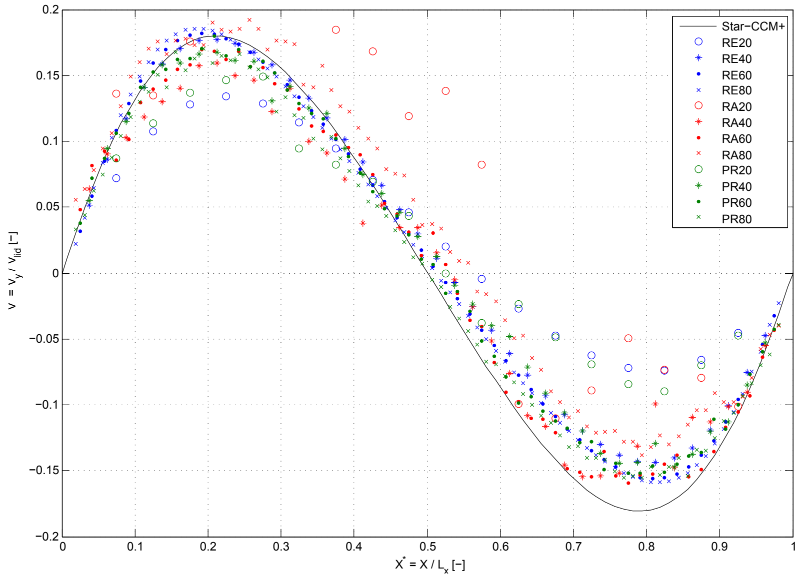

Figure 4: Non-dimensional vertical velocities along the horizontal centreline of the cavity: regular (RE), pseudo-random (PR) and random (RA).

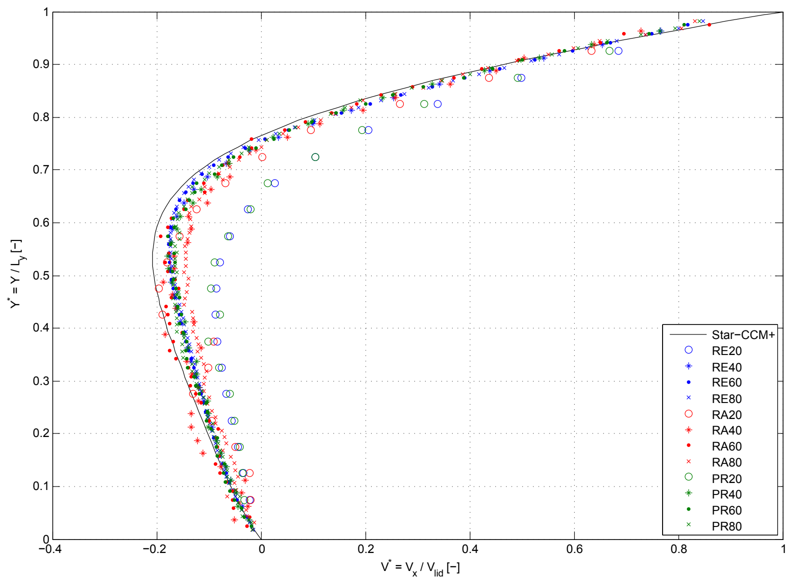

Figure 5: Non-dimensional horizontal velocities along the vertical centreline of the cavity: regular (RE), pseudo-random (PR) and random (RA).

[4] Colagrossi, A. *A Meshless Lagrangian Method for Free-Surface and Interface with Fragmentation.* Ph.D. Thesis. Università di Roma La Sapienza, Rome (2003).

[5] Monaghan, J. J. Smoothed particle hydrodynamic simulations of shear flow. *Mon. Not. R. Astron. Soc.* (2006) **365**(1):199–213.

[6] Imaeda, Y. and Inutsuka, S.-I. Shear Flows in Smoothed Particle Hydrodynamics. *Astrophys. J.* (2002) **569**(1):501–518.

[7] Price, D. J. Smoothed particle hydrodynamics and magnetohydrodynamics. *J. Comput. Phys.* (2012) **231**(3):759–794.

[8] Cartwright, A., Stamatellos, D. and Whitworth, A. P. The effect of Poisson noise on SPH calculations. *Mon. Not. R. Astron. Soc.* (2009) **395**(4):2373–2380.

[9] Hubber, D. A., Falle, S. A. E. G. and Goodwin, S. P. Convergence of AMR and SPH simulations - I. Hydrodynamical resolution and convergence tests. *Mon. Not. R. Astron. Soc.* (2013) **432**:711–727.

[10] Lucy, L. B. A numerical approach to the testing of the fission hypothesis. *Astron. J.* (1977) **82**(12).

[11] Gingold, R. A. and Mon, J. J. Smoothed particle hydordynamics: theory and application to non-spherical stars. *Mon. Not. R. Astron. Soc.* (1977) **181**:375–389.

[12] Liu, M. B. and Liu, G. R. Smoothed Particle Hydrodynamics (SPH): An Overview and Recent Developments. *Arch. Comput. Methods Eng.* (2010) **17**:25–76.

[13] Galagali, N. *Algorithms for Particle Remeshing Applied to Smoothed Particle Hydordynamics*. MA Thesis. Massachusetts Institute of Technology (2009).

[14] Liu, G. R. and Liu, M. B. *Smoothed Particle Hydrodynamics — A Meshfree Particle Method.* World Scientific Publishing (2003).

[15] Liu, M. B., Liu, G. R. and Lam, K. Y. Constructing smoothing functions in smoothed particle hydrodynamics with applications. *J. Comput. Appl. Math.* (2003) **155**:263–284.

[16] Monaghan, J. J. Why Particle Methods Work. *SIAM J. Sci. Comput.* (1982) **3**(4):422-433.

[17] Kim, J and Moin, P. Application of a fractional-step method to incompressible Navier Stokes equations. *J. Comput. Phys.* (1985) **59**(2):308–323.

[18] Schreiber, R and Keller, H. Driven cavity flows by efficient numerical techniques. *J. Comput. Phys.* (1983) **49**(2):310–333.